

RESEARCH PAPER

Role of *Rubia tinctorum* in the synthesis of zinc oxide nanoparticles and apoptosis induction in breast cancer cell line

Zahra Shamasi ¹, Ali Es-haghi ^{1*}, Mohammad Ehsan Taghavizadeh Yazdi ², Mohammad Sadegh Amiri ³, Masoud Homayouni-Tabrizi ¹

¹Department of Biology, Mashhad Branch, Islamic Azad University, Mashhad, Iran

²Medical Toxicology Research Center, School of Medicine, Mashhad University of Medical Sciences, Mashhad, Iran

³Department of Biology, Payame Noor University, Tehran, Iran

ABSTRACT

Objective(s): Nowadays, nanotechnology has offered great success in resolving concerns in cancer therapy and created a new interdisciplinary field of study incorporating various sciences, such as biology, chemistry and medicine. Apoptosis is a conserved and controlled strategy in regulating cellular growth and proliferation, as well as preserving development and general homeostasis of the body. Zinc oxide nanoparticles (ZnO-NPs) are the most important and widely used nanoparticles. This study aimed to evaluate the apoptosis-inducing properties of the synthesized ZnO-NPs by aqueous extract of *Rubia tinctorum* against the MCF7 breast cancer cell line.

Materials and Methods: Zinc oxide nanoparticles were synthesized using *Rubia tinctorum* extract and characterized by some methods including dynamic light scattering (DLS), field emission scanning electron microscopy (FESEM) and x-ray diffraction analysis (XRD). Apoptosis was measured by the Hoechst and Acridine-Orange/Propidium Iodide staining, as well as flow cytometry.

Results: The results of this study showed that the particle size of biosynthesized ZnO-NPs using *R. tinctorum* extract was about 40 nm and had a spherical morphology. The obtain results of the Hoechst and Acridine-Orange/Propidium Iodide staining, as well as flow cytometry showed that biosynthesized ZnO-NPs effectively and dose-dependently induced apoptosis in the MCF7 breast cancer cells.

Conclusion: Therefore, the biosynthesized ZnO-NPs by watery extract of *R. tinctorum* can be used in the treatment of many diseases, including cancers.

Key Words: Apoptosis, Breast cancer, Green Synthesis, *Rubia tinctorum*, zinc oxide nanoparticles

How to cite this article

Shamasi Z, Es-haghi A, Taghavizadeh Yazdi ME, Amiri MS, Homayouni-Tabrizi M. Role of *Rubia tinctorum* in the synthesis of zinc oxide nanoparticles and apoptosis induction in breast cancer cell line. *Nanomed J.* 2021; 8(1): 65-72. DOI: 10.22038/nmj.2021.08.07

INTRODUCTION

Nanotechnologies are supplying a long range to define the qualities of the material in a novel technique of eco-friendly and biologic-synthetic way [1-5]. Zinc-Oxide nanoparticles (ZnO-NPs) are well-known for their safe and biologically compatible properties [6]. They can be utilized as anticancer factors [7], drug delivery agents [8], antimicrobials [9], and bio-sensors [10] due to their remarkable physicochemical assets. Zinc is a biologically compatible element in humans, which plays several roles in the body. There are various

fabrication ways of metal-oxide NPs, the majority of which are toxic and expensive [11, 12]. The ZnO-NPs have extensive applications particularly in the field of sensors, wastewater treatments, and biomedical tools [13-15].

The utilization of plant materials for the green synthesis of nanoparticles has evolved in the last decade [16]. Plants contain certain bioactive compounds, such as flavonoids, phenols, alcoholic-sugars, terpenes, alkaloids, and reductase, which act as reducing agents [17-19]. Plant-mediated synthesis of nanoparticles is a very promising area of nanotechnology since the plant itself acts as both a reducing and capping agent [20, 21]. The plant system can synthesize nanoparticles

* Corresponding Author Email: ashaghi@gmail.com

Note. This manuscript was submitted on July 9, 2020; approved on October 27, 2020

both intracellularly and extracellularly [22]. Green approaches of the ZnO-NPs synthesis are environmentally friendly, cheap, and easy to administer [23-25]. It is recognized that medicinal plants are rich in phenols, flavonoids, and carbohydrates which have antioxidant potential [17, 18, 20, 26]. Additionally, it is described that synthesized NPs using herbal medicine exhibited extra antioxidant properties [27, 28]. Various plants, such as *Deverra tortuosa* [29], *Aloe socotrina* [30], *Eucalyptus globules* [31], and *Melia azedarach* [32] have been used in the synthesis of zinc oxide nanoparticles so far.

Apoptosis is a conserved and controlled strategy to eliminate unnecessary and potentially harmful cells in living organisms. This process interacts with the immune system and participates in the pathogenesis of many diseases [33]. Apoptosis also shows a key role in imperative bio-processes, such as evolution, homeostasis, as well as the removal of virus-infected and self-reactive immune cells, especially T lymphocytes [34]. This process is very important in regulating cellular growth and proliferation, as well as preserving development and general homeostasis of the body [35]. Apoptosis is involved in the pathogenesis of many autoimmune diseases, cancers, and infections, as well as tissue repair and regeneration [36]. A decreased rate of apoptosis can lead to the growth of cancer cells or the development of autoimmune disorders. Conversely, an increased rate of apoptosis is observed in diseases, such as neurodegenerative disorders and acquired immunodeficiency syndrome [37].

The ZnO-NPs are among the most important and widely used nanoparticles to cope with different infections in many countries and the medical and pharmaceutical industries [38]. Therefore, the current study aimed to elucidate a green methodology of *Rubia tinctorum* root extract for the biosynthesis of ZnO-NPs. The biosynthesized nanoparticles were further characterized using a particle size analyzer, a field emission scanning electron microscopy (FESEM), and X-ray diffraction (XRD). In addition, the apoptotic properties of the ZnO-NPs using different methods were evaluated in this study.

MATERIALS AND METHODS

Materials

Zinc acetate was obtained from Merck, and deionized water was employed to prepare all the

required solutions. Moreover, *Rubia tinctorum* was obtained from a local source (Mashhad-Iran).

Biosynthesis of ZnO-NPs by aqueous root extract of *Rubia tinctorum*

Initially, 10 g of *Rubia tinctorum* was put on a Hot Plate Stirrer and immersed in 100 ml distilled water for 1 hr at 40°C. Subsequently, it was filtered through a filter paper, and 10 ml of the plant extract was mixed with 100 ml of zinc acetate (9 g of zinc acetate with 100 ml of distilled water) and placed on a hot plate for 3 hr at 40°C.

Characterization techniques

The biosynthesized ZnO-NPs were characterized by a particle size analyzer, dynamic light scattering (DLS), FESEM, and XRD techniques. Briefly, the distribution size of the nanoparticles was studied by the Zetasizer instrument (Malvern, UK), and the FESEM (JEOL, Japan) was employed to detect the shape of the ZnO-NPs. The crystal construction and purity of the ZnO-NPs were established by XRD. In the next stage, the biosynthesized ZnO-NPs were centrifuged (8000 rpm, 30 minutes), washed, and dried to remove the non-binding.

Acridine Orange/Propidium Iodide staining

The utilization of Acridine Orange (AO) and Propidium Iodide (PI) as fluorescent dyes is an easy and fast way to discern living cells from non-living ones. This method was performed to determine the number of apoptotic cells in nanoparticle-treated and negative control groups. Initially, 5 ml cell suspension containing 1 million cells was cultured in flasks for 24 hr. Afterward, the medium was removed, and the cells were handled with diverse concentrations of nanoparticles for 48 h. Subsequently, the cells were centrifuged at 2700 rpm (5 min), and after removing the supernatant, the cell pellet was diluted with 1 ml Phosphate Buffered Saline (PBS). In the next step, 10 µl of the cell suspension was admixed with 10 µl AO and 10 µl PI and incubated for 5 min at 37°C. Following that, 20 µl of the resulting mixture was poured on a slide, and a lamella was placed above the slide. Finally, the sample was photographed and studied using the fluorescence microscopy [39].

Hoechst staining

The cells were washed with PBS and fixed in 1% formaldehyde solution to investigate the morphology of the apoptotic cells by fluorescence

microscopy and after treatment with various concentrations of NPs for 24 hr. The cells were then immersed in pure methanol for 20 min. The methanol was removed by centrifugation, and the cells were again washed with PBS. After preparing slides from the cells, they were examined for morphological signs of apoptosis by fluorescence microscopy (ZEISS, Germany). Apoptotic cells were characterized by morphological changes of the nucleus (e.g. the presence of dense chromatin fragments) [40, 41].

Flow-cytometry assay

Flow cytometry was applied to determine apoptosis by evaluating the changes in the cell cycle. This is a method widely used in research and clinical settings for identifying cells and evaluating their properties. In the flow cytometry, various cells are identified based on their light scattering and fluorescence emission properties. Fluorescence emission can be obtained using fluorescent dyes, such as PI. First, the cells were cultured in 6-well plates and exposed to various concentrations of nanoparticles. Afterward, the cells were washed with PBS and treated with PI (30 min). Finally, the cells were isolated and subjected to flow cytometry analysis to determine the ratios of the cells in different cell-cycle phases [40].

Catalase gene expression assay

Catalase gene expression was specified in the MCF-7 cell line treated with nanoparticles. The cells were seeded at 5×10^3 cells/ml in a 6-well plate using RPMI media treated with the concentrations of nanoparticle including 0, 30, 40, and 50 $\mu\text{g/ml}$, and incubated for 48 hr. The treated cells were then washed with PBS. Table 1 tabulates the characteristics of the primer.

Table 1. Primer characteristics employed for the investigation of catalase gene expression

Gene		Sequences (5' to 3')
CAT	F	CGTGCTGAATGAGGAACAGA
	R	AGTCAGGGTGGACCTCAGTG
GAPDH	F	CGTGCTGAATGAGGAACAGA
	R	AGTCAGGGTGGACCTCAGTG

Real-Time polymerase chain reaction method

The catalase gene expression was determined using the Real-Time Polymerase Chain Reaction method (Qiagen Rotor-Gene Q, Hilden, Germany). Amplification status was set as a primary step at 95°C (2 min), followed by 30 cycles of 95°C

(15 sec), 56.4°C (20 sec), and 72°C (30 sec). Melting curves were created by monitoring the fluorescence of the SYBR green signal from 65°C to 95°C. Comparative ΔCt normalized to GAPDH (glyceraldehyde 3-phosphate dehydrogenase) was used to calculate transcription levels using the geNorm algorithm automated in CFX manager software (Bio-Rad).

Statistical analysis

All data collected from this study were analyzed in SPSS software using ANOVA. The significance was certified by Duncan's multiple range tests. A p-value less than 0.05 was considered statistically significant. All tests were performed triplicate, and the results are shown as mean \pm SD.

RESULTS

Characterization of the ZnO-NPs

The DLS was conducted to define the typical size of the ZnO-NPs, and the results are revealed in Fig 1.

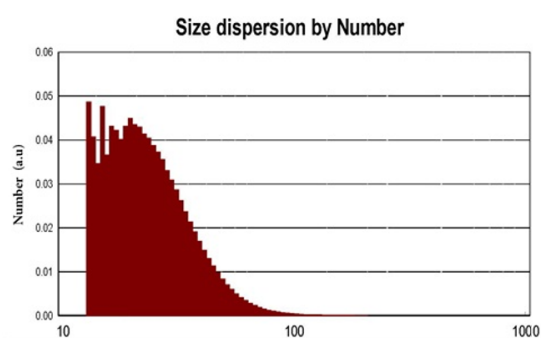


Fig 1. Size dispersion of the synthesized ZnO-NPs using *Rubia tinctorum*

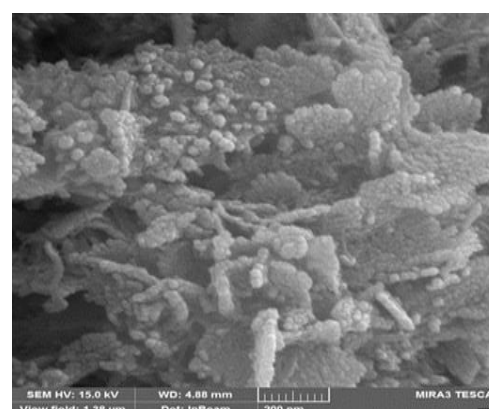


Fig 2. FESEM images of the synthesized ZnO-NPs using *Rubia tinctorum*

The particle size distribution of the ZnO-NPs ranged from 10 to 70 nm. Moreover, the mean particle size was about 40 nm. The field emission and transmission electron microscopy were performed to characterize the construction things of the NPs. The ZnO-NPs were imagined by FESEM, and the results revealed that the ZnO-NPs had a spherical morphology, and some were in an aggregated form (Fig 2). Fig 3 illustrates the XRD patterns of the ZnO-NPs synthesized by *Rubia tinctorum* extract. The XRD pattern shows peaks at $2\theta=31.67^\circ$, 34.31° , and 36.14° that assigned to (100), (002), and (101), respectively, representing the polycrystalline wurtzite structure of the NPs.

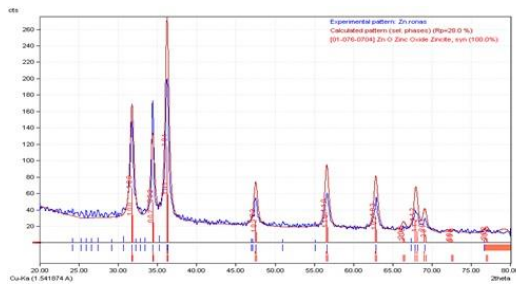


Fig 3. XRD pattern of the biosynthesized ZnO-NPs using *Rubia tinctorum*

Apoptotic morphological changes include cell contraction, nucleus fragmentation, and chromatin condensation, which can be visualized by light or fluorescent microscopy.

In this study, AO/PI and Hoechst staining, as well as flow cytometry were used to determine apoptosis.

Moreover, the up-regulation of the catalase gene was utilized to determine the molecular mechanism of the apoptotic pathway.

Study of apoptosis using Acridine Orange/Propidium Iodide staining

To investigate apoptosis by AO/PI staining, the cultured MCF7 cells treated with ZnO-NPs were stained with fluorescent AO and PI, and the apoptosis was assessed by the fluorescent microscopy.

As illustrated in Fig 4, green cells in the control group indicate no apoptosis after 24 hr of incubation. In contrast, most nanoparticle-treated cells showed yellow, orange, and red colors indicating the induction apoptosis in these cells.

The results also showed that apoptosis-inducing activity was augmented with increasing concentration of ZnO-NPs.

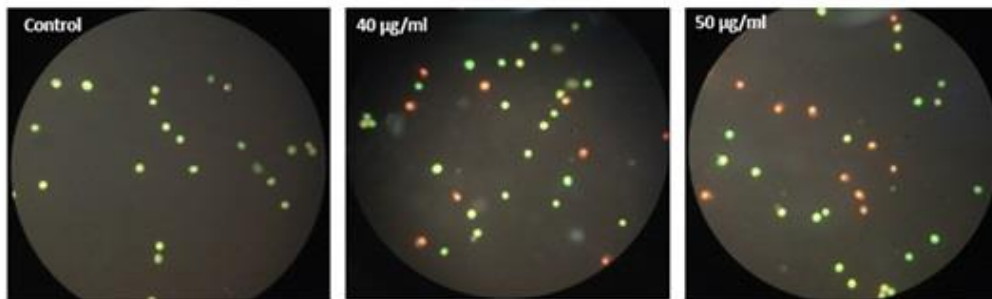


Fig 4. Effect of zinc oxide nanoparticles on the morphological composition of MCF-7 cells treated with concentrations of 40 and 50 µg/ml, compared to the group control, using the Acridine-Orange test. The green color represents the living cells; however, yellow and red cells represent the apoptotic cell (200 x magnification)

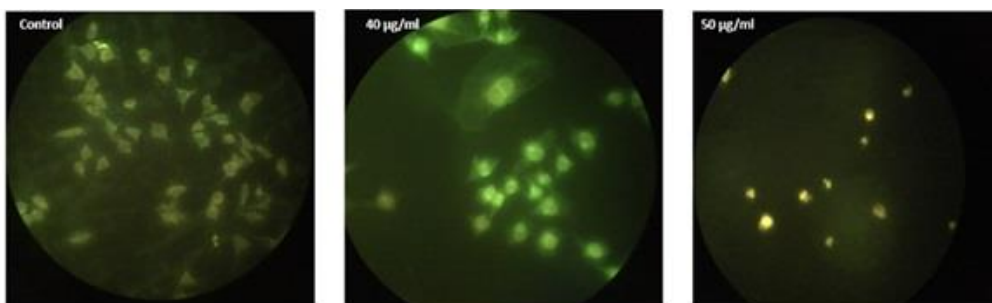


Fig 5. Hoechst Staining of MCF-7 cells treated with concentrations of 40 and 50 µg/ml, compared to the control group (200 x magnification)

Evaluation of apoptosis by hoechst staining

The MCF-7 cells were stained with Hoechst fluorescent dye after being exposed to various doses of ZnO-NPs for 24 hr. Apoptosis was examined by fluorescent microscopy. This dye was absorbed by apoptotic cells treated with ZnO-NPs and brightened their nucleus. As indicated in Fig 5, no changes were observed in the luminosity of the control cells. The apoptosis induction activity of the nanoparticles was dose-dependent.

Evaluation of the apoptosis and cell-cycle changes by flow cytometry

The MCF-7 cell treatment with concentrations of ZnO-NPs was performed for 24 hr using a flow cytometer assay. The findings showed a significant and dose-dependent increase in the ratio of the cells in the SubG1 phase of the cell cycle in the cells treated with ZnO-NPs, compared to the control group (Fig 6).

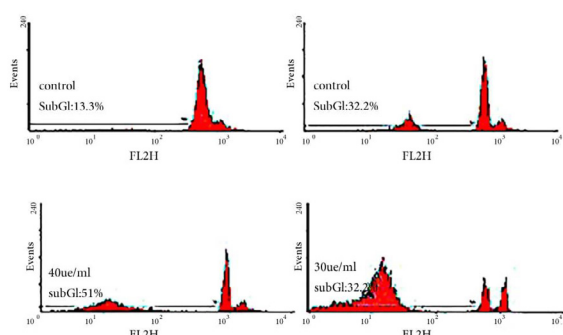


Fig 6. Flow cytometry analysis of apoptosis in MCF-7 breast cancer cells treated with different concentrations of ZnO-NPs. Apoptosis was significantly increased in the cells treated with different concentration of ZnO-NPs, compared to the control group

As shown in Fig 6, at the dose of 30, 40, and 50 µg / mL, cells in the SubG1 phase are 32%, 51%, and 80%, respectively, which also reflects the effects of the dosage of the nanoparticle. This observation indicated increased apoptosis in these cells by increasing the dosage of the nanoparticle.

Up-regulation of catalase gene expression

Catalase gene expression changes were investigated in the MCF-7 cells treated with ZnO-NPs produced from aqueous extract of *Rubia tinctorum*. The results showed that the expression of the catalase gene in the MCF-7 cells treated with different concentrations of ZnO-NPs up to 50 µg/ml was significantly increased. As shown in Fig 7, the expression level of the CAT gene at

a concentration of 50 µg/ml was increased by approximately 30-fold, compared to the control group. This data suggest that ZnO-NPs induce reactive oxygen species (ROS) production within the cell resulting in increased expression of the catalase gene to remove these species. It can be concluded that biosynthesized ZnO-NPs may induce apoptosis through increased ROS production.

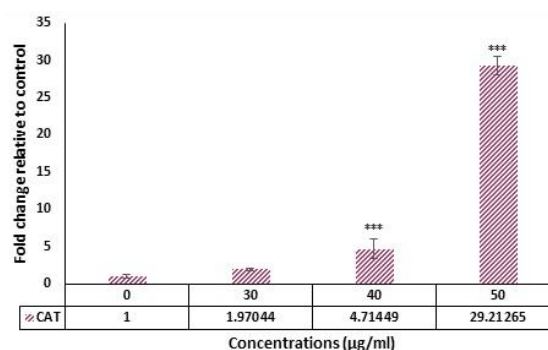


Fig 7. Expression analysis of the catalase gene in the MCF-7 cells upon treatment with 0, 30, 40, and 50 µg / ml of CeO₂-NP for 24 h. ***P<0.001 indicates a significant difference, compared to the control group (0)

DISCUSSION

Apoptosis is a well-defined model of cell death which varies in morphology, mechanisms, and occurrence from the other cell death, such as necrosis [42]. Since apoptosis is a controlled process, its incidence in cancer therapy has great considerations. Because of this, apoptosis is the primary target in many cancer treatment strategies [43, 44]. Apoptosis is the potential process of the MCF-7 cell death after subjecting to the ZnO-NPs. The ZnO-NPs have been described to have apoptotic effects against cancer cells. This study investigated the effects of ZnO-NPs on the MCF-7 breast cancer cell line and showed that these nanoparticles could selectively induce apoptosis in the cancer cells. Through several experiments, it was revealed that ZnO-NPs synthesis via the green method by *Rubia tinctorum* root extract induce the apoptosis in the MCF-7 cells after 24 hr. The degree of apoptosis is improved by increasing the ZnO-NPs concentration. A similar study showed that the ZnO-NPs could induce apoptosis in mouse neural stem cells [45]. Therefore, ZnO-NPs may be potentially helpful in the treatment of breast cancer. In another study, the effects of ZnO-NPs on the induction of oxidative stress and apoptosis were investigated in human colon carcinoma cells

[46]. In a recently conducted study, the toxicity of the nanoparticles was measured by the MTT assay, and apoptosis was evaluated using the flow cytometry showing a cell death rate of 98%. In the current study, the ZnO-NPs were synthesized by the extract of *R. tinctorum* plant, and the results revealed acceptable toxicity against MCF-7 cancer cells with an IC50 of about 40 µg / ml at 24 h.

Another study investigated the influence of ZnO-NPs on the induction of DNA destruction, oxidative stress, and apoptosis in malignant A375 melanoma cells. The IC50 of the ZnO-NPs was estimated at 20 µg/ml using the MTT assay in the recent report [47]. On the other hand, the IC50 of the ZnO-NPs against MCF-7 breast cancer cells was obtained at 40 µg/ml in the present study indicating lower cytotoxicity against breast cancer cells. Furthermore, these nanoparticles were comparably effective in inducing apoptosis and DNA destruction in breast and melanoma cancer cells. In another study, ZnO-NPs were shown to induce apoptosis and oxidative stress in human lung LTP-a-2 cells. Apoptosis was identified by fluorescent microscopy and Caspase 3 activity test [48]. It has been noted that ZnO-NPs promote toxicity and apoptosis mainly through inducing ROS production in human lung adenocarcinoma cells [49]. This observation provides valuable information regarding the action mechanism of the nanomaterials in cancer therapy. In another study, the applicability of ZnO-NPs was analyzed in targeted and synergistic (i.e. along with other chemotherapeutics) cancer therapies. In this study, the biomedical and clinical applications of metal and ZnO-NPs have been reviewed *in vitro* [50]. In addition, the benefits, methods, and limitations of using metallic oxide NPs in cancer treatment and drug delivery have been discussed focusing on ZnO-NPs and their cytotoxic mechanisms as well as tactics to increase their targeting and cell toxicity against cancer cells [51-53].

The above-mentioned studies show that ZnO-NPs synthesized by plant extracts present cytotoxicity against cancer cells and can activate apoptosis in them. Therefore, they can be used as anticancer compounds.

CONCLUSION

Nanotechnology refers to the knowledge of production and application of materials with 1 to 100 nm dimensions. Moreover, it is the investigation of the exclusive physical, chemical,

and biological properties to be applied in clinical settings. Nowadays, nanotechnology has offered great success in resolving concerns in cancer therapy and created a new interdisciplinary field of study incorporating various sciences, such as biology, chemistry, and medicine. The apoptotic activity of ZnO-NPs synthesized by aqueous extract of *R. tinctorum* was investigated against the MCF7 breast cancer cell line by staining and flow cytometry methods. The results showed that these nanoparticles were capable of inducing morphological changes (e.g. abnormal shape and nucleation) in the cancer cells. Flow cytometry analysis showed that the ratio of cells in the SubG1 phase of the cell cycle was increased in cells treated with the ZnO-NPs indicating the elevated rate of apoptosis.

Regarding the useful properties of the ZnO-NPs synthesized by the aqueous extract of *R. tinctorum*, it can be said that these particles can be used in the treatment of many diseases, including cancer, as well as other biomedical fields.

ACKNOWLEDGMENTS

The authors would like to thank the Mashhad Branch, the Islamic Azad University of Mashhad for the provided chemicals and laboratory facilities.

REFERENCES

1. Hamidi A, Yazdi MET, Amiri MS, Hosseini HA, Darroudi M. Biological synthesis of silver nanoparticles in *Tribulus terrestris* L. extract and evaluation of their photocatalyst, antibacterial, and cytotoxicity effects. *Res Chem Intermed.* 2019; 45(5): 2915-2925.
2. Yazdi MET, Khara J, Sadeghnia HR, Bahabadi SE, Darroudi M. Biosynthesis, characterization, and antibacterial activity of silver nanoparticles using *Rheum turkestanicum* shoots extract. *Res Chem Intermed.* 2018; 44(2): 1325-1334.
3. Taghavizadeh Yazdi ME, Hamidi A, Amiri MS, Kazemi Oskuee R, Hosseini HA, Hashemzadeh A, et al. Eco-friendly and plant-based synthesis of silver nanoparticles using *Allium giganteum* and investigation of its bactericidal, cytotoxicity, and photocatalytic effects. *Mater Technol.* 2019; 34(8): 490-497.
4. Yazdi MET, Khara J, Housaindokht MR, Sadeghnia HR, Bahabadi SE, Amiri MS. Role of *Ribes khorassanicum* in the biosynthesis of AgNPs and their antibacterial properties. *IET Nanobiotechnol.* 2018; 13(2): 189-192.
5. Zarei M, Karimi E, Oskoueian E, Es-Haghi A, Yazdi MET. Comparative Study on the Biological Effects of Sodium Citrate-Based and Apigenin-Based Synthesized Silver Nanoparticles. *Nutr Cancer.* 2020: 1-9.
6. Zabih E, Babaei A, Shahrampour D, Arab-Bafrani Z, Mirshahidi KS, Majidi HJ. Facile and rapid in-situ synthesis of chitosan-ZnO nano-hybrids applicable in medical purposes; a novel combination of biomineralization, ultrasound, and bio-safe morphology-conducting agent.

- Int J Bio. Macromol. 2019 (131): 107-116.
7. Alavi-Tabari SA, Khalilzadeh MA, Karimi-Maleh H. Simultaneous determination of doxorubicin and dasatinib as two breast anticancer drugs uses an amplified sensor with ionic liquid and ZnO nanoparticle. *Journal of electroanalytical chemistry*. 2018(811): 84-88.
 8. Einafshar E, Haghghi Asl A, Malekzadeh A. Synthesis of new biodegradable nanocarriers for SN38 delivery and synergistic phototherapy. *Nanomed J*. 2018; 5(4): 210-216.
 9. Mohamadian F, Eftekhari L, Haghghi Bardineh Y. Applying GMDH artificial neural network to predict dynamic viscosity of an antimicrobial nanofluid. *Nanomed J*. 2018; 5(4): 217-221.
 10. Shetti NP, Bukkitgar SD, Reddy KR, Reddy CV, Aminabhavi TM. ZnO-based nanostructured electrodes for electrochemical sensors and biosensors in biomedical applications. *Biosens Bioelectron*. 2019; 141: 111417.
 11. Es-haghi A, Javadi F, Yazdi MET, Amiri MS. The Expression of Antioxidant Genes and Cytotoxicity of Biosynthesized Cerium Oxide Nanoparticles Against Hepatic Carcinoma Cell Line. *Avicenna J Med. Biochem*. 2019; 7(1): 16-20.
 12. Javadi F, Yazdi MET, Baghani M, Es-haghi A. Biosynthesis, characterization of cerium oxide nanoparticles using *Ceratonia siliqua* and evaluation of antioxidant and cytotoxicity activities. *Mater Res Express*. 2019; 6(6): 065408.
 13. Zhu L, Zeng W. Room-temperature gas sensing of ZnO-based gas sensor: A review. *Sensor Actuat A-Phys*. 2017; 267: 242-261.
 14. Ani I, Akpan U, Olutoye M, Hameed B. Photocatalytic degradation of pollutants in petroleum refinery wastewater by TiO₂- and ZnO-based photocatalysts: recent development *J Clean Prod*. 2018; 205: 930-954.
 15. Jiang J, Pi J, Cai J. The advancing of zinc oxide nanoparticles for biomedical applications. *Bioinorg Chem Appl*. 2018; 2018.
 16. Sharifan H, Moore J, Ma X. Zinc oxide (ZnO) nanoparticles elevated iron and copper contents and mitigated the bioavailability of lead and cadmium in different leafy greens. *Ecotoxicol. Environ. Saf*. 2020; 191: 110177.
 17. Yazdi MET, Khara J, Husaindokht MR, Reza H, Sadeghnia SEB, Amiri MS. Biocomponents and antioxidant activity of *Ribes khorasanicum*. *IJBMS*. 2018; 3(3): 99-103.
 18. Yazdi T, Ehsan M, Housaindokht MR, Sadeghnia HR, Esmailzadeh Bahabadi S, Amiri MS. Assessment of phytochemical components and antioxidant activity of *Rheum turkestanicum* Janisch. *Studies in Medical Sciences*. 2020; 31(2): 75-81.
 19. Rahnama M, Johnson R, Voisey C, Simpson W, Fleetwood D. The global regulatory protein Vela Is required for symbiosis between the endophytic fungus *Epichloë festucae* and *Lolium perenne*. *Mol Plant Microbe Interact*. 2018; 31(6): 591-604.
 20. Darroudi M, Yazdi MET, Amiri MS. Plant-Mediated Biosynthesis of Nanoparticles. *21st Century Nanoscience—A Handbook*: CRC Press; 2020. p. 1-18.
 21. Yazdi MET, Amiri MS, Hosseini HA, Oskuee RK, Mosawee H, Pakravanan K, et al. Plant-based synthesis of silver nanoparticles in *Handelia trichophylla* and their biological activities. *Bull Mater Sci*. 2019; 42(4): 155.
 22. Rai M, Yadav A. Plants as potential synthesiser of precious metal nanoparticles: progress and prospects. *IET Nanobiotechnol*. 2013; 7(3): 117-124.
 23. Saad AM, Abukhadra MR, Ahmed SA-K, Elzanaty AM, Mady AH, Betiha MA, et al. Photocatalytic degradation of malachite green dye using chitosan supported ZnO and Ce-ZnO nano-flowers under visible light. *J Environ Manage*. 2020; 258: 110043.
 24. Liu X, Li X, Liu X, He S, Jin J, Meng H. Green preparation of Ag-ZnO-rGO nanoparticles for efficient adsorption and photodegradation activity. *Colloid Surface A*. 2020; 584: 124011.
 25. Chauhan AK, Katarina N, Garg V. Green fabrication of ZnO nanoparticles using *Eucalyptus* spp. leaves extract and their application in wastewater remediation. *Chemosphere*. 2020; 247: 125803.
 26. Modarres M, Bahabadi SE, Yazdi MET. Enhanced production of phenolic acids in cell suspension culture of *Salvia leriifolia* Benth. using growth regulators and sucrose. *Cytotechnology*. 2018:1-10.
 27. Aseyd Nezhad S, Es-haghi A, Tabrizi MH. Green synthesis of cerium oxide nanoparticle using *Origanum majorana* L. leaf extract, its characterization and biological activities. *Appl Organomet Chem*. 2020; 34(2): e5314.
 28. Noohpisheh Z, Amiri H, Farhadi S, Mohammadi-gholami A. Green synthesis of Ag-ZnO nanocomposites using *Trigonella foenum-graecum* leaf extract and their antibacterial, antifungal, antioxidant and photocatalytic properties. *Spectrochim Acta A*. 2020: 118595.
 29. Selim YA, Azb MA, Ragab I, Abd El-Azim MH. Green Synthesis of Zinc Oxide Nanoparticles Using Aqueous Extract of *Deverra tortuosa* and their Cytotoxic Activities. *Sci Rep*. 2020; 10(1): 1-9.
 30. Fahimmunisha BA, Ishwarya R, AlSalhi MS, Devanesan S, Govindarajan M, Vaseeharan B. Green fabrication, characterization and antibacterial potential of zinc oxide nanoparticles using *Aloe socotrina* leaf extract: A novel drug delivery approach. *J Drug Deliv Sci Technol*. 2020; 55: 101465.
 31. Ahmad H, Venugopal K, Rajagopal K, De Britto S, Nandini B, Pushpalatha HG. Green synthesis and characterization of zinc oxide nanoparticles using *Eucalyptus globules* and their fungicidal ability against pathogenic fungi of apple orchards. *Biomolecules*. 2020; 10(3): 425.
 32. Dhandapani KV, Anbumani D, Gandhi AD, Annamalai P, Muthuvenkatachalam BS, Kavitha P. Green route for the synthesis of zinc oxide nanoparticles from *Melia azedarach* leaf extract and evaluation of their antioxidant and antibacterial activities. *Biocatal Agric Biotechnol*. 2020; 24: 101517.
 33. Goldar S, Khaniani MS, Derakhshan SM, Baradaran B. Molecular mechanisms of apoptosis and roles in cancer development and treatment. *Asian Pac J Cancer Prev*. 2015; 16(6): 2129-2144.
 34. Marsden VS, Strasser A. Control of apoptosis in the immune system: Bcl-2, BH3-only proteins and more. *Annu Rev Immunol*. 2003; 21(1): 71-105.
 35. Hipfner DR, Cohen SM. Connecting proliferation and apoptosis in development and disease. *Nat Rev Mol Cell Biol*. 2004; 5(10): 805-815.
 36. Favaloro B, Allocati N, Graziano V, Di Ilio C, De Laurenzi V. Role of apoptosis in disease. *Aging (Albany NY)*. 2012 ;4(5): 330.
 37. Behl C. Apoptosis and Alzheimer's disease. *J Neural Transm*. 2000; 107(11): 1325-1344.
 38. Król A, Pomastowski P, Rafińska K, Railean-Plugaru V,

- Buszewski B. Zinc oxide nanoparticles: Synthesis, antiseptic activity and toxicity mechanism. *Adv Colloid Interfac.* 2017; 249: 37-52.
39. Bank HL. Rapid assessment of islet viability with acridine orange and propidium iodide. *In Vitro Cell Dev Biol.* 1988; 24(4): 266-273.
40. Oancea M, Mazumder S, Crosby ME, Almasan A. Apoptosis assays. *Cardiovascular Disease: Springer*; 2006. p. 279-290.
41. Crowley LC, Marfell BJ, Waterhouse NJ. Analyzing cell death by nuclear staining with Hoechst 33342. *Cold Spring Harb. Protoc.* 2016;2016(9):pdb. prot087205.
42. Dive C, Gregory CD, Phipps DJ, Evans DL, Milner AE, Wyllie AH. Analysis and discrimination of necrosis and apoptosis (programmed cell death) by multiparameter flow cytometry. *Biochim Biophys Acta (BBA)-Molecular Cell Research.* 1992; 1133(3): 275-285.
43. Burz C, Berindan-Neagoe I, Balacescu O, Irimie A. Apoptosis in cancer: key molecular signaling pathways and therapy targets. *Acta Oncol.* 2009; 48(6): 811-821.
44. Plati J, Bucur O, Khosravi-Far R. Apoptotic cell signaling in cancer progression and therapy. *Integr Biol.* 2011; 3(4): 279-296.
45. Deng X, Luan Q, Chen W, Wang Y, Wu M, Zhang H. Nanosized zinc oxide particles induce neural stem cell apoptosis. *Nanotechnology.* 2009; 20(11): 115101.
46. De Berardis B, Civitelli G, Condello M, Lista P, Pozzi R, Arancia G. Exposure to ZnO nanoparticles induces oxidative stress and cytotoxicity in human colon carcinoma cells. *Toxicol. Appl. Pharmacol.* 2010; 246(3): 116-127.
47. Saud Alarifi DA, Alkahtani S, Verma A, Ahamed M, Ahmed M, Alhadlaq HA. Induction of oxidative stress, DNA damage, and apoptosis in a malignant human skin melanoma cell line after exposure to zinc oxide nanoparticles. *Int J Nanomedicine.* 2013; 8: 983.
48. Wang C, Hu X, Gao Y, Ji Y. ZnO nanoparticles treatment induces apoptosis by increasing intracellular ROS levels in LTP-a-2 cells. *Biomed Res Int.* 2015; 2015.
49. Wang C, Wang H, Lin M, Hu X. ZnO nanoparticles induced cytotoxicity on human pulmonary adenocarcinoma cell line LTP-a-2. *Process Saf Environ Prot.* 2015; 93: 265-273.
50. Guo D, Wu C, Jiang H, Li Q, Wang X, Chen B. Synergistic cytotoxic effect of different sized ZnO nanoparticles and daunorubicin against leukemia cancer cells under UV irradiation. *J Photochem Photobiol B Biol.* 2008; 93(3): 119-126.
51. Wilczewska AZ, Niemirowicz K, Markiewicz KH, Car H. Nanoparticles as drug delivery systems. *Pharmacol Rep.* 2012; 64(5): 1020-1037.
52. Albanese A, Tang PS, Chan WC. The effect of nanoparticle size, shape, and surface chemistry on biological systems. *Annu Rev Biomed Eng.* 2012; 14: 1-16.
53. Yao J, Yang M, Duan Y. Chemistry, biology, and medicine of fluorescent nanomaterials and related systems: new insights into biosensing, bioimaging, genomics, diagnostics, and therapy. *Chem Rev.* 2014; 114(12): 6130-6178.